Research Repository UCD

Title	Influence of ageing on the structure and phosphate adsorption capacity of dewatered alum sludge
Authors(s)	Yang, Y., Zhao, Y.Q., Kearney, P.
Publication date	2008-12-15
Publication information	Yang, Y., Y.Q. Zhao, and P. Kearney. "Influence of Ageing on the Structure and Phosphate Adsorption Capacity of Dewatered Alum Sludge." Elsevier, December 15, 2008. https://doi.org/10.1016/j.cej.2008.04.026.
Publisher	Elsevier
Item record/more information	http://hdl.handle.net/10197/3138
Publisher's statement	This is the author's version of a work that was accepted for publication in Chemical Engineering Journal. Changes resulting from the publishing process, such as peer review, editing, corrections, structural formatting, and other quality control mechanisms may not be reflected in this document. Changes may have been made to this work since it was submitted for publication. A definitive version was subsequently published in Chemical Engineering Journal, 145 (2): 276-284 DOI 10.1016/j.cej.2008.04.026.
Publisher's version (DOI)	10.1016/j.cej.2008.04.026

Downloaded 2026-05-01 23:38:17

The UCD community has made this article openly available. Please share how this access benefits you. Your story matters! (@ucd_oa)

© Some rights reserved. For more information

Influence of ageing on the structure and phosphate adsorption capacity of dewatered alum sludge

Y. Yang, Y. Q. Zhao*, P. Kearney

Centre for Water Resources Research, School of Architecture, Landscape and Civil Engineering, Newstead Building, University College Dublin, Belfield, Dublin 4, Ireland

---

* **Corresponding author:**

Dr Y. Q. Zhao

Centre for Water Resources Research

School of Architecture, Landscape and Civil Engineering

Newstead Building

University College Dublin

Belfield

Dublin 4, Ireland

Tel: +353-1-7163215; Fax: +353-1-7163297

E-mail: yaqian.zhao@ucd.ie

Abstract

In line with the increasing studies on the beneficial reuse of alum sludge from a "waste" into useful raw material, this paper reports an in-depth investigation of the effects of ageing time on the structure and the phosphate adsorption capacity of a dewatered alum sludge obtained from a local drinking water treatment plant in Ireland. During the ageing period from 0 day to up to 18 months, the adsorption capacity of the sludge varied from 21.4 to 23.9 mg-P g^{-1}-sludge at pH 4.3, 14.3 to 14.9 mg-P g^{-1}-sludge at pH 7.0 and 0.9 to 1.1 mg-P g^{-1}-sludge at pH 9.0, respectively, indicating marginal effect of ageing time on such sludge's ability to adsorb phosphate. This result seems conflict with other studies reported in the literature. To reveal such, series of investigations including physicochemical characterization, morphological structure, BET surface area and porous structure of the aged sludge were carried out. All the results conclusively show that ageing time has insignificant effect on the structure and properties of the dewatered alum sludge and thus the phosphate adsorption capacity of the alum sludge remains insignificant change during the ageing.

Key words

Alum sludge; Adsorption; Phosphorus removal; Ageing time; Pore structure; Surface area

1. Introduction

Phosphorus (P) is an essential nutrient for the growth of aqueous plants and is also a principal element to cause eutrophication in the water environment. Generally, the biological phosphorus removal (BPR) process and/or chemical precipitation are used in the removal of P from wastewater. In chemical removal, lime and metal salts, such as aluminium, iron and magnesium salts are used for this purpose [1]. However, this can increase the operational costs and/or sludge production, thus hindering its widespread use. Therefore, other cost effective treatment methods and materials are being investigated. Alum sludge is an inevitable by-product of the production of drinking water when aluminium salt is added as a coagulant. In Ireland, as in most other countries worldwide, alum sludge is historically reviewed as 100 % "waste" and disposed of in landfill sites. However, following sustainability principles, there is a progressive drive towards alum sludge reuse as a beneficial material. In particular, previous work done by investigators including the authors showed that alum sludge has a considerable adsorption capacity and can be utilized as a low-cost adsorbent for P immobilization from wastewaters and contaminated soils [2-9].

Factors to influence P adsorption capacity of alum sludge are mainly derived from two catalogues. One is from the sources/processes of the sludge to be formed, such as source water quality, dose of alum salt and other chemicals, water treatment process etc. [3] and the other is from the P-sorption testing conditions, such as particle size, equilibrium time, initial P concentration [2,5,10,11]. Furthermore, ageing time of the sludge appears to affect the P sorption capacity as well. DeWolfe [3] reported that the ability of alum sludge to bind P is likely due to a multitude of factors including the age of the sludge. It is claimed that the old/aged alum sludge is likely to be less reactive due to mineralization of aluminium. Compared with aluminium hydroxides, alum sludge may have different but similar

77 characteristics in structure and P adsorption mechanism. Amorphous aluminium hydroxide,
78 which is thermodynamically metastable, can be transformed to thermodynamically stable
79 phases with increasing ageing time, pH and temperature [12]. The path of structural
80 transformation could be different with various mobility of ions that are related to the water
81 content [13]. In the ageing process under aqueous condition, it was reported that the
82 Brunauer-Emmett-Teller (BET) surface area of aluminium hydroxide floc formed from
83 aluminium sulphate addition to lake waters, was decreased from 72 m^2 g^{-1} (at 4 days of
84 ageing) to 38 m^2 g^{-1} (at 120 days) and was accompanied by the transformation of amorphous
85 $Al(OH)_3$ to gibbsite which increases the crystallinity of the aluminium hydroxide floc [14].
86 The significant decrease of the surface area of the floc over ageing time is believed to be
87 related to the structural transformation [14-16]. The P adsorption capacity of aluminium
88 hydroxide floc aged for 6 months was about 50 % lower than the fresh floc; this is likely due
89 to the alterability of the structural transformations and the reactivity of P adsorption [14].
90 During the ageing process under dry conditions, however, structural transformation does
91 occur, but at lower rates since the ion mobility is restricted [13]. It was reported that alum
92 sludge showed no significant change in the structure, adsorption sites and P adsorption
93 capacity despite ageing of the sludge in the laboratory for approximately 5 years [17].
94 Interestingly, aluminium hydroxide sample prepared at 70 ^oC showed a significant decrease
95 in surface area and micropore volume within the first month of ageing was also reported [6].
96 Although the sludge samples were collected from different locations and the experimental
97 conditions might be different, the conflicting results emphasize the need for a more detailed
98 and in-depth study into the effect of the ageing time on structure and the P capacity of the
99 alum sludge. This forms the basis of the present study.
100 Noting that whether ageing affects the P adsorption capacity of alum sludge depends on the
101 influence of the ageing time on the structure and surface properties of alum sludge. The

objectives of this study were to (1) identify the effect of ageing time on P adsorption capacity of dewatered alum sludge and (2) characterize the structure and the surface properties of alum sludge during the ageing process of up to 18 months.

2. Materials and methods

2.1. Source of dewatered alum sludge and sample preparation

Dewatered alum sludge cakes were collected from an industrial filter press of the sludge dewatering unit of the Ballymore Eustace Water Treatment Plant, Co. Kildare, Ireland. The plant produces about 230,000 to 275,000 m^3 d^{-1} of potable water for Dublin city. The raw water with a mean colour of 105 Hazen units flows through a series of tunnels under gravity from the Poulaphuca reservoir, 1.5 km away from the plant. Aluminium sulphate is used as the primary chemical coagulant at a dose of 42-60 mg L^{-1}. After collection, the sludge cakes (moisture content 72 ~ 75 %) were stored at room temperature in a well-covered container for a period of up to 18 months, during which the samples of sludge stored for 0 day (fresh alum sludge), 6, 12, and 18 months were subjected to various tests for their chemical properties, P-adsorption capacities and structures. It should be pointed out that, to eliminate the affect of air-drying process on the moisture content of the sludge, the sludge was stored in a well-covered environment, causing the anaerobic condition of the sludge during ageing process. However, the potential effects of anaerobic condition on the structure and properties of alum sludge were not considered in the current study. Before tests at each specific ageing time, the sludge samples were taken from the storage and air-dried at room temperature for 1 week. The sludge was then ground and sieved to provide the test adsorbent with diameter < 0.063 mm.

2.2. Chemical characterization of the alum sludge

The prepared alum sludge samples at each ageing time were dried in an oven at 103 ± 2 ^{o}C for 72 hours to determine the moisture content. The 103 ± 2 ^{o}C dried samples were weighed and digested using the standard method of nitric acid digestion (3030 E) [18]. Thereafter, the chemical composition of the samples was examined using Inductively Coupled Plasma-Optical Emission Spectrum (ICP-AES, IRIS Intrepid II XSP, Thermo Elemental, Franklin, Massachusetts, USA), Ion Chromatography (DX-120, Dionex, Sunnyvale, California, USA) and Total Organic Carbon (TOC)-V_{CSH} (Shimadzu, Tokyo, Japan).

2.3. Adsorption capacity

Adsorption capacity of the sludge sample at each specific ageing period was determined using batch tests. Different masses of the alum sludge ranging from 0.2 to 20.0 g L^{-1} were prehydrolyzed in a pH controlled distilled water (pH 4.3 to 9) for 48 h. Thereafter, standard aliquots of the P stock solution, which were prepared by dissolving pre-weighed potassium dihydrogen phosphate (KH_2PO_4) in distilled water, were then introduced, giving a resultant initial P concentration of 100 mg-P L^{-1}, and alum sludge content ranged from 0.1 to 10.0 g L^{-1}. The mixtures were then mechanically agitated to enhance adsorption over a 48 hours equilibration period that was pre-determined in the previous study [4]. During this period, the solution was adjusted to the required pH (ranged from 4.3 to 9.0) using sulphuric acid (0.01 M) and sodium hydroxide (0.1 M). After adsorption, equilibrated samples were filtered using 0.45 *μm* millipore filter paper (Millipore, Billerica, Massachusetts, USA) and analysed for P concentration using the stannous chloride method (4500-P D) [18]. The equilibrium

adsorption capacities were calculated from a linearized form of the Langmuir adsorption isotherm [19].

$$\frac{C_e}{q} = \frac{1}{Q_0} C_e + \frac{1}{Q_0 b} \quad (1)$$

where q is the mass of P adsorbed per unit mass of sludge(mg-P g^{-1}sludge); C_e is the equilibrium concentration of phosphate in the suspension (mg-P L^{-1}); Q_0 is the maximum adsorption capacity (mg-P g^{-1}sludge); b is the constant related to the energy of the adsorption-desorption process with unit of inverse of concentration C_e. By plotting C_e vs. C_e/q, a straight line with slope $1/Q_0$ is obtained and the Q_0 can be calculated.

2.4. Morphological and structural characterization

2.4.1. Morphological structure and functional group characterization

The morphology of each sludge sample at different ageing time was examined by scanning electron microscope (SEM, JSM-6700F, Japan Electron Optics Laboratory, Tokyo, Japan) and X-ray powder diffraction (XRD, D/max-3C, Rigaku, Tokyo, Japan). The functional group of the sludge was also examined by Attenuated Total Reflectance Fourier Transform Infrared (ATR-FTIR) (EQUINOX-55, Bruker, Ettingen, Germany).

2.4.2. BET surface area and pore structure

Low temperature nitrogen adsorption-desorption isotherms. To determine the surface area and the pore characteristics of the alum sludge, the prepared sample (air-dried, particle diameter < 0.063 mm) was outgassed at 250 ± 5 ^oC for 3 hours until the relative pressure (p/p^0) was less than 10^{-6}. Thereafter, low temperature nitrogen adsorption-desorption isotherms at 77.4 ± 0.1 K were conducted using a Surface Area and Pore Size Analyzers (SA3100, Beckman Coulter, Fullerton, California, USA).

175

176 *BET surface area.* The BET surface area was calculated by fitting the nitrogen adsorption
177 isotherm data to the BET model [20] (see Equations 2, 3&4).

$$\frac{p/p^0}{n(1-p/p^0)} = \frac{1}{n_m c} + \frac{c-1}{n_m c}(p/p^0) \quad (2)$$

$$A_{BET} = 4.35 n_m, \quad n_m = \frac{1}{s+i} \quad (3)$$

$$c = \frac{s}{i} + 1 \quad (4)$$

178 where p/p^0 is the relative pressure; n is the volume of the gas adsorbed at p/p^0 (ml(STP) g^{-1});
179 n_m is the monolayer adsorption capacity (ml(STP) g^{-1}); c is the BET constant which is
180 approximately equal to $e^{(E_l-E_L)/RT}$ (E_l is the heat of adsorption of the gas in the first adsorbed
181 layer, and E_L is the heat of liquefaction of the gas); A_{BET} is the specific surface area calculated
182 from BET model.

183

184 *Mesopore pore size distribution.* The mesopore size distribution was obtained from the
185 desorption branch of the low temperature nitrogen isotherm using the method of Pierce [21].
186 The hysteresis loop range used for pore size distribution was from p/p^0=0.948 to 0.445 (fresh
187 sample), 0.956 to 0.434 (6 months old sample), 0.948 to 0.465 (12 months old sample), and
188 0.957 to 0.45 (18 months old sample), respectively.

189

190 *Micropore and micropore surface area.* The micropore identification was carried out and the
191 micropore surface areas of the alum sludges were examined using the *t*-plot. *t*-plot is a plot of
192 the isotherm with the statistical thickness of the film (*t*). Fitting the linearized Harkins-Jura
193 (HJ) model (see Equation 5) to the experimental data, the constants *a* and *b* can be
194 determined [22]. Thereafter, *t* is determined by using the HJ equation (see Equation 6). In the

range $t \leq 3.54$ Å, the slope of the straight line can be used to obtain the surface area (indicated as $A_{t,HJ}$) and this can be use as criteria to test the correctness of the pore type identification model. In the range $t > 3.54$ Å, the slope of the straight line gives the mesopore surface area (indicated as $A_{t,HJ,Meso}$) of the adsorbent. The difference between $A_{t,HJ}$ and $A_{t,HJ,Meso}$, gives the surface area contributed by micropore (if the micropore is present) [23,24].

$$\log(p/p^0) = b - \frac{a}{(n/n_m)^2} \quad (5)$$

$$t = 3.54\left[\frac{a}{b - \log(p/p^0)}\right]^{\frac{1}{2}} \text{ (Å)} \quad (6)$$

Where 3.54 Å corresponds to the thickness of the nitrogen layer [25].

3. Results

3.1. Chemical composition of the alum sludge

The quantitative chemical composition of the alum sludge at different ageing times is given in Table 1. The dominant component in all the sludge samples is aluminium (as Al_2O_3) with approximately 424.3, 430.4, 418.9 and 436.7 mg g^{-1}-sludge in 0 day, 6, 12 and 18 months' storage, respectively. In spite of some scatter, the insignificant change of the aluminium content (in the range from -1.3 % to 2.9 %) during the ageing period studied was observed. The moisture content of the samples of 0 day, 6, 12 and 18 months' ageing time is 34.6 %, 24.7 %, 25.3 % and 24.6 %, respectively. This shows similarity in free-water content of the sludges under different ageing time, especially after 6 months. The mass loss at 500 ^oC is due to the loss of volatile organic matter and also part of the structural hydroxyl ion. At 1000 ^oC, the mass loss is caused by the loss of structural hydroxyl ion. Overall, the striking feature of

the data in Table 1 lies in the insignificant difference in the chemical characteristics of the sludge throughout the 18 months ageing period, which shows considerable stability in its chemical characteristics.

[Table 1 The chemical components of the fresh alum sludge (ageing time: 0 day) and the aged alum sludge (ageing time: 6, 12 and 18 months)]

3.2. Effect of ageing time on P adsorption capacity

The effect of the ageing time on P adsorption capacity of the alum sludge at different pH conditions is shown in Fig. 1. The maximum adsorption capacity, Q_0, obtained using Langmuir isotherm, in 18 months ageing varied 21.4 ~ 23.9 (at pH 4.3), 17.7 ~ 19.1 (at pH 6.0), 14.3 ~ 14.9 (at pH 7.0), 1.1 ~ 1.7 (at pH 8.5) and 0.9 ~ 1.1 mg-P g^{-1}-sludge (at pH 9.0). These results clearly show that the adsorption capacity of the alum sludge decreases with increasing pH, this respect has been examined in our earlier studies [4,5]. It is however more important to note that the ageing seems not to considerably affect the P-adsorption capacity of the alum sludge since the change < 5 % in maximum adsorption capacity during the ageing process was statistically obtained.

[Fig. 1. P adsorption capacity of the alum sludge at different ageing times and pH condition]

3.3. Effect of ageing time on sludge structural characteristics

3.3.1. Solid-phase structural transformation

Fig. 2 illustrates the X-ray diffraction patterns of the fresh and aged sludges. It can be seen clearly that the fresh and aged sludges exhibit quite similar XRD characteristics. There is no considerable crystalline-aluminium related XRD peak observed. This indicates that crystallization (a process of transformation of amorphous form to crystalline) did not occur during the ageing process. In contrast, the XRD pattern elucidates the amorphous structure of the alum sludge. The peak in Fig. 2 is identifiable crystalline solid of silicon oxide (SiO_2), which can be identified by the powder diffraction file (PDF).

[Fig. 2. X-ray diffraction patterns of alum sludge at various ageing times]

3.3.2. Functional groups on the surface of the aged sludges

Fig. 3 shows the ATR-FTIR spectra of the alum sludge at different ageing times. The comparison of ATR-FTIR spectra can reveal the transformation (if any) of the hydroxyl group (–OH) on surface of alum sludge at different ageing times. The surface hydroxyl group is essentially related to the adsorption capacity of the alum sludge due to the fact that the functional group plays a dominant role in the ligand exchange mechanism of the P-adsorption onto the surface of alum sludge [5]. The OH vibration detected in the ATR-FTIR spectra of the sludge can reveal any transformation of the OH group on the alum sludge. The bonded OH stretching vibration can be detected at ca. 3400 (3600-3200) cm^{-1} (antisymmetric and symmetric OH stretching mode) and 1625 (1650-1600) cm^{-1} (HOH bending mode) [26,27]. From Fig. 3, it can be seen that the spectrum is characterized by a broad peak which is due to functional group vibration at 3427 and 1618 cm^{-1} for all the sludge samples, irrespective of their ageing time. The main adsorption band in the spectrum of the alum sludge appeared at 3427 cm^{-1} and this can be identified as the OH group due to its vibration [27,28], while the absorption at 1618 cm^{-1} can be potentially linked to the bonded OH and/or organic functional

group (i.e. C=C, C=N) [29,30]. Notwithstanding the ageing time, the intensity of the OH and/or C=C and C=N vibration did not change. The similar characteristics of the ATR-FTIR of the different aged sludge samples, as shown in Fig. 3, lead to the conclusion that there was no transformation of functional groups during the ageing process. This implies that the ageing time did not affect any change of the functional group (-OH and/or humic substances) on the surface of the alum sludge.

[Fig. 3. ATR-FTIR spectra of alum sludge samples with different ageing times]

3.3.3. BET surface area of the aged sludges

The BET plots of the aged alum sludges, which were obtained through applying Equation (1) to experimental data, are presented in Fig. 4. The n_m, BET *c*-constant and surface area (A_{BET}) can be calculated from the BET model and the results are shown in Table 2. The A_{BET} of the alum sludge at different ageing times is respectively 49.03 (0 day, fresh alum sludge), 62.33 (6 months), 54.60 (12 months), and 53.54 m^2 g^{-1}-sludge (18 months). This indicates that the surface area of alum sludge was not decreased with the ageing time. In contrast, a considerable increase of the surface area at 6 months was observed. Although there was some difference in the surface area of the samples, this is rather caused by sample differences (see Table 1) and not particularly due to the effect of the ageing time. It is also noted in Table 2 that the value of BET *c*-constant for the different alum sludge samples is approximately the same, while the monolayer adsorption capacity (n_m) did not differ significantly. This indicates that there was no significant change in surface properties of alum in spite of their different ageing time.

[Fig. 4. BET plots of low temperature nitrogen adsorption isotherm of the fresh alum sludge (ageing time: 0 day) and the aged alum sludges (ageing time: 6, 12 and 18 months)]

[Table 2 Results of BET plot using nitrogen adsorption isotherm of the fresh alum sludge (ageing time: 0 day) and the aged alum sludges (ageing time: 6, 12 and 18 months)]

3.3.4. Porous structure of the aged alum sludges

The nitrogen adsorption-desorption isotherm is presented in Fig. 5. From the adsorption branch, the isotherm of the alum sludge represents Type IV according to the Brunauer-Deming-Deming-Teller (BDDT) classification [31], while the desorption branch exhibits a wide hysteresis loop. The hysteresis loop refers to a phenomenon in which the desorption isotherm curve does not coincide with the adsorption isotherm curve. This is caused by the fact that the nitrogen released during the desorption process is always less than the amount of nitrogen adsorbed during the adsorption over the high relative pressure range, a phenomenon caused by the condensation in the pores or capillaries. The hysteresis loop occurred over the entirely high relative pressure range, i.e. at p/p^0=0.445-0.991 (0 day, fresh alum sludge); 0.434-0.99 (6 months); 0.465-0.989 (12 months) and 0.45-0.99 (18 months), which represents the capillary condensation. The very similar trends of the hystersis loops of the different samples clearly indicate the unchanged porous structure of the sludge during the ageing time tested.

[Fig. 5. Nitrogen adsorption-desorption isotherms at 77.4 K for different ageing times of alum sludges]

3.4. SEM observation of the aged alum sludges

Fig. 6 (a-d) shows the SEM images of the alum sludge at different ageing times. The presence of the cylindrical-like shape, mesosize pores (which are several tens of nanometres in diameter) in the alum sludges can be observed from Fig. 6. More importantly, from the comparison of the SEM images, the very similar amorphous structures of the sludges can be observed despite their different ageing times. Both the morphological structure, pore size and the pore shape remain unchanged during the ageing process. This further proves the non-structural transformation during the ageing process, although the SEM provides a qualitative description.

[Fig. 6. SEM images of the fresh alum sludge (ageing time: 0 day) and the aged alum sludges (ageing time: 6, 12 and 18 months)]

4. Discussion

4.1. Effect of ageing time on structural transformation

In considering the use of alum sludge as a low cost adsorbent for P immobilization, the need for detailed investigation of ageing effect on its P adsorption ability is a crucial necessity in both academic and practical respects. It is believed that the adsorption capacity of alum sludge depends on the chemical nature of the sludge. Any changes of its chemical characteristics and related structure and surface properties during the sludge ageing process will be useful to identify and understand the change (if any) of its P adsorption ability. Current evidence from literature seems to reveals some conflict as regards this. In an evaluation of the influence of ageing time on P adsorption capacity of aluminium hydroxide

floc, it was shown that approximately 20 % of the floc had transformed to gibbsite after 20 days and over 70 % was transformed in 180 days ageing time [14]. More recently, Georgantas and Grigoropoulou [32] provided the evidence on XRD monitoring of aluminum hydroxide during ageing. It has been demonstrated that the characteristic diffraction band of gibbsite appeared in the second month of ageing and this diffraction band become sharper with time. Accordingly, the P sorption capacity was reported to decrease with the structural transformation. One possible reason could be the decrease of the non-structural –OH, due to its transformation into the structural –OH during the ageing process of aluminium hydroxide. The result in the decrease of available ligand exchangeable ion subsequently leads to the decrease in P adsorption capacity [16,33]. It is important to note that the above claims of the structural transformation of the aluminium hydroxide (flocs) were based on the ageing in aqueous condition. However, in an artificial ageing process (both thermal and wet and dry incubation) of a relative dry condition of alum sludge amended soils, Agyin-Birikorang and O'Connor [34] investigated the lability of alum sludge immobilized phosphorus and reported that P would remain immobilized and was no release in the long term. Also in dry ageing condition, this study revealed that the amorphous structure of the alum sludge (see Fig. 2) did not change into the thermodynamically stable structure (crystalline) during 18 months. The cause of this is likely due to the fact that such structural changes are kinetically very slow especially in dry conditions [35], although they are certainly thermodynamically possible. In addition, the presence of organic acid [36] and/or ionic strength may slow this process [16,37]. Consequently, the unchanged surface structure and functional group of alum sludge can be suggested as reasons for the insignificantly changed P-adsorption capacity (see Fig. 1).

4.2. Effect of ageing time on surface area

In a study of P adsorption on alum hydrolysis products, it was reported the transformation of amorphous aluminium hydroxide to crystalline form and this transformation was accompanied by a decrease of surface area over the ageing time [38]. This may affect the reactivity of the aluminium hydrolysis products and the availability of the surface area that are crucial for P adsorption. As a result, the adsorption capacity was decreased during the ageing period [14,36]. However, the examination on the surface area of the aged sludges in this study (Fig. 4) provides hard evidences to support the fact of insignificant change of surface area during the ageing process. It is believed that the surface area must be sufficient enough to accommodate the P molecules located on the surface of the alum sludge. This is particularly important as most of the surface area is located in the interior of the alum sludge particle. Therefore, any significant decrease in the surface area of alum sludge during the ageing period can reduce the adsorption capacity. Therefore, the unchanged surface area can be attributed as reasons for the unchanged adsorption capacity (see Fig. 1).

4.3. Effect of ageing time on pore size distribution and pore type

4.3.1. Effect of ageing time on pore size distribution

The pore type and the pore size of alum sludge are crucial for P adsorption since alum sludge should provide enough pathway through which the adsorbate molecules can gain access into the interior of the alum sludge particle. Therefore, any significant change in pore type and the pore size during the ageing process can result in the change of the sludge adsorption capacity.

A characteristic feature of mesopore solid is that its adsorption isotherm represents Type IV with a hysteresis loop [39]. The Type IV adsorption isotherm and the hysteresis loop in the adsorption-desorption isotherm of the current study indicate clearly the existence of the mesoporous structure of the alum sludge (Fig. 5). From the SEM images, the presence of

cylindrical-like mesopore can be qualitatively seen in various aged sludge samples (see Fig. 6).

To further characterize the structural change in term of pore size distribution during the ageing process, a comparative quantitative method is applied to reveal the porous structure and its change in more detail. The mesopore size distribution based on surface area is shown in Fig.7. The main feature of this illustration is a very similar characterization in pore size distribution with different ageing times of the sludge. Fifty percent of the surface area of the ageing sludges is contributed by pores with sizes less than 5.98 (0 day), 6.13 (6 months), 6.10 (12 months) and 6.17 nm (18 months), while ninety percent of surface area is contributed by pores of size less than 9.67 (0 day), 9.01 (6 months), 9.39 (12 months) and 9.60 nm (18 months). The pores with sizes larger than 20 nm only contributed insignificant amount to the surface area. The slight difference in pore size distribution between the ageing sludges is most likely due to sample differences rather than the ageing time. Accordingly, the unchanged surface area can be attributed as reason for the unchanged adsorption capacity (see Fig.1)

[Fig. 7. Mesopore surface area-pore size distribution of the fresh alum sludge (ageing time: 0 day) and the aged alum sludges (ageing time: 6, 12 and 18 months)]

4.3.2. Effect of ageing time on pore type

In addition, to reveal the entire porous structure and characteristics of the alum sludge, *t*-plot can be employed to reveal both qualitative and quantitative information about the micropore [23]. For the non-porous solid, the *t*-plot is a straight line through the entire multilayer adsorption range and the straight line through the origin. For the porous solid, the straight line can be obtained in the low pressure range. The difference between the *t*-plot straight line and

414 the *t*-curve can be used to characterize the presence or otherwise of a certain type of pore
415 [23,40,41]. The *t*-curve, as shown in Fig. 8, exhibits a downward deviation from the straight
416 line. This is observable in the fresh alum sludge (ageing time: 0 day) only.
417
418 [Fig. 8. *t*-plot of the fresh alum sludge (ageing time: 0 day) (using HJ model and HJ *t*-
419 equation)]
420
421 The upward deviation of *t*-curve from the straight line, as shown in Fig. 9, suggests that
422 there are no micropores in the 6, 12 and 18 months old samples. From the intercept of the *t*-
423 plot, the presence or otherwise of the micropores can be quantitatively and qualitatively
424 determined. From the comparison of the porous structure based on the *t*-plot, it can be noted
425 that the only porous structural change during the ageing process is the disappearance of the
426 micropores in the alum sludge. The micropore surface area in the fresh sample (ageing time:
427 0 day) is 15.31 m^2/g-sludge and this represents 31.41% of the entire surface area (see Table
428 3). The comparison of the surface area obtained through the BET model (A_{BET}) (see Table 2)
429 and the t_{HJ}-plot ($A_{t,HJ}$) (see Table 3) shows that the $A_{t,HJ}$ is 0.57 % (0 day), 0.87 % (6 months),
430 2.31 % (12 months) and 2.07 % (18 months) lower than A_{BET}. The good agreement between
431 A_{BET} and $A_{t,HJ}$ shows the validity of using HJ model and HJ *t*-equation to characterize the
432 pore type of the aged alum sludges.
433
434 [Fig. 9. *t*-plot of 6, 12 and 18 months aged alum sludge (using HJ model and HJ *t*-equation)]
435
436 [Table 3 Harkins-Jura model constants and t_{HJ}-plot results of the fresh alum sludge (ageing
437 time: 0 day) and the aged alum sludges (ageing time: 6, 12 and 18 months)]
438

Overall, the approaches used to reveal the chemical composition, morphological structure, surface functional group, surface area, pore type and pore distribution, which are believed to highly relevant in affecting the adsorption ability of alum sludge, support the idea of inconsiderable change in the P adsorption capacity of dewatered alum sludge over ageing time. The adsorption capacity of the alum sludge, being 'ageing time-independent', is almost definitely due to its 'unchanged' chemical and structural characteristics with ageing time.

5. Conclusions

The results of this study provide insight and concrete evidence to demonstrate the stability of the structure and surface characteristics of the alum sludge over time. It further provides basis to the unexpected change in P-adsorption capacity of alum sludge over time. Despite the inherent variability of the alum sludge samples, the results of SEM, XRD, ATR-FTIR, nitrogen adsorption-desorption isotherm, surface area, pore area and pore size distribution indicated that the ageing time has no significant effects on the structure and surface characteristics. The major conclusions of this study are:

- Results of SEM and XRD show that solid-phase transformation did not occur during the 18 months ageing process. Although the alum sludge has an amorphous structure, which is thermodynamically metastable, there was no morphological structural transformation observed in the aged sludge. This indicates that the influence of ageing time on the structure and surface properties of alum sludge is different from that of pure aluminium hydrolysis products because the two solid phases have totally different chemical characteristics and composition. In addition, transformation of the aged alum sludge into more stable forms is not observed and this is adduced to be a combination of

464 the kinetic behaviour, environmental conditions and/or the presence of other inhibiting
465 materials.
466 ● The ATR-FTIR result indicates that the functional group on the surface of the alum
467 sludge did not change over the ageing time.
468 ● The BET surface of the aged sludges did not decrease during the ageing process. The
469 type of low temperature nitrogen adsorption-desorption isotherm and the SEM images
470 indicate that the alum sludge is structurally mesoporous. The t_{HJ}-plot results illustrate that
471 the fresh alum sludge (ageing time: 0 day) contains micopores while for the 6, 12 and 18
472 months aged sludge there was no micropore being observed. This is likely thought to be
473 due to the extended ageing time which may control the entirely mesoporous structure of
474 the alum sludge. Results of the mesopore size distributions also show that the alum sludge
475 samples have a similar size distribution with a narrow pore size distribution. There was
476 no significant change over the ageing time.
477 ● The findings of the current investigation are vital for two main reasons: (1) Aside from
478 revealing the in-depth phenomena of the ageing process of alum sludge, it provides useful
479 information on the implication of the reuse of alum sludge as adsorbent for P removal
480 when the alum sludge is stored over a long time; (2) From the engineering point of view,
481 the unchanged adsorption capacity is crucial in ensuring a sustainable pathway for the
482 reuse of the alum sludge in environmental engineering applications.
483

484 **Acknowledgements**

485

486 The authors gratefully acknowledge financial support received from the EPA (Ireland)
487 through the Environmental Technologies Scheme (Project No. 2005-ET-S-7-M3), and also
488 technical support received from the University College Dublin (UCD), Ireland and the Xi'an

University of Architecture and Technology, PR China. Authors also wish to sincerely acknowledge the valuable comments and remarks of the anonymous reviewers.

References

[1] D. Jenkins, J.F. Ferguson, A.B. Menar, Chemical processes for phosphate removal, Water Res. 5 (7) (1971) 369-389.

[2] M. Razali, Y.Q. Zhao, M. Bruen, Effectiveness of a drinking-water treatment sludge in removing different phosphorus species from aqueous solution, Sep. Purif. Technol. 55 (3) (2007) 300-306.

[3] J. DeWolfe, Water residuals to reduce soil phosphorus, IWA Publishing, London, UK, 2006.

[4] Y. Yang, D. Tomlinson, S. Kennedy, Y.Q. Zhao, Dewatered alum sludge: a potential adsorbent for phosphorus removal, Water Sci. Technol. 54 (5) (2006) 207-213.

[5] Y. Yang, Y.Q. Zhao, A.O. Babatunde, L. Wang, Y.X. Ren, Y. Han, Characteristics and mechanisms of phosphate adsorption on dewatered alum sludge, Sep. Purif. Technol. 51 (2) (2006) 193-200.

[6] K.C. Makris, W.G. Harris, G.A. O'Connor, H. El-Shall, Long-term phosphorus effects on evolving physicochemical properties of iron and aluminum hydroxides, J. Colloid Interface Sci. 287 (2) (2005) 552-60.

[7] J.G. Kim, J.H. Kim, H. Moon, C. Chon, J.S. Ahn, Removal capacity of water plant alum sludge for phosphorus in aqueous solution, Chem. Speciation Bioavailability 14 (2002) 67-73.

514 [8] S.H. Huang, B. Chiswell, Phosphate removal from wastewater using spent alum sludge,
515 Water Sci. Technol. 42 (3-4) (2000) 295-300.
516 [9] H. Roques, L. Nugroho-Jeudy, A. Lebugle, Phosphorus removal from wastewater by half-
517 burned dolomite, Water Res. 25 (8) (1991) 959-965.
518 [10] S. Tanada, M. Kabayama, N. Kawasaki, T. Sakiyama, T. Nakamura, M. Araki, T.
519 Tamura, Removal of phosphate by aluminum oxide hydroxide, J. Colloid Interface Sci.
520 257 (1) (2003) 135-140.
521 [11] H. Stefan, Mechanisms of phosphorus stabilization in the soil environment: A molecular
522 scale evaluation. PhD dissertation, University of Delaware, Newark, Delaware, USA,
523 2003.
524 [12] K. Okada, T. Nagashima, Y. Kameshima, A. Yasumori, T. Tsukada, Relationship
525 between formation conditions, properties and crystallite size of boehmite, J. Colloid
526 Interface Sci. 253 (2) (2002) 308-314.
527 [13] U. Schwertmann, J. Friedl, H. Stanjek, From Fe (III) ions to ferrihydrite and then to
528 hematite, J. Colloid Interface Sci. 209 (1) (1999) 215-223.
529 [14] J. Berkowitz, M.A. Anderson, C. Amrhein, Influence of aging on phosphorus sorption to
530 alum floc in lake water, Water Res. 40 (5) (2006) 911-916.
531 [15] J. Berkowitz, M.A. Anderson, R. Graham, Laboratory investigation of aluminum
532 solubility and solid-phase properties following alum treatment of lake waters, Water Res.
533 39 (16) (2005) 3918-3928.
534 [16] J.T. Sims, B.G. Ellis, Changes in phosphorous sorption associated with aging of
535 aluminum hydroxide suspensions, Soil Sci. Soc. Am. J. 47 (5) (1983) 912-916.
536 [17] K.C. Makris, Long-term stability of sorbed phosphorus by drinking water treatment
537 residuals: Mechanisms and implications, PhD Dissertation, University of Florida,
538 Gainesville, Florida, USA, 2004.

539 [18] APHA, AWWA, WEF, Standard methods for the examination of water and wastewater
540 (18th edition), Washington DC, USA, 1992.
541 [19] G. Tchobanoglous, F.L. Burton, H.D. Stensel, Wastewater Engineering: Treatment and
542 Reuse (Fourth edition), McGraw-Hill, London, UK, 2003.
543 [20] S. Brunauer, P.H. Emmett, E. Teller, Adsorption of gases in multimolecular layers, J.
544 Am. Chem. Soc., 60 (2) (1938) 309-319.
545 [21] C. Pierce, Computation of pore sizes from physical adsorption data, J. Phys. Chem. 57 (2)
546 (1953) 149-152.
547 [22] W.D. Harkins, G. Jura, Surfaces of Solids XIII. A vapor adsorption method for the
548 determination of the area of a solid without the assumption of a molecular area, and the
549 areas occupied by nitrogen and other molecules on the surface of a solid, J. Am. Chem.
550 Soc. 66 (8) (1944) 1366-1373.
551 [23] R.S. Mikhail, S. Brunauer, E.E. Bodor, Investigations of a complete pore structure
552 analysis I. Analysis of micropores, J. Colloid Interface Sci. 26 (1) (1968) 45-53.
553 [24] B.C. Lippens, J.H. de Boer, Studies on pore systems in catalysts V. The t method, J.
554 Catal. 4 (3) (1965) 319-323.
555 [25] B.C. Lippens, B.G. Linsen, J.H. de Boer, Studies on pore systems in catalysts I. The
556 adsorption of nitrogen: apparatus and calculation, J. Catal. 3 (1) (1964) 32-37.
557 [26] J.R. Ferraro, Low-frequency vibrations of inorganic and coordination compounds,
558 Plenum Press, New York, USA, 1971.
559 [27] J.H. van der Maas, Basic Infrared Spectroscopy (Second edition), Heyden & Son Ltd.,
560 London, UK, 1972.
561 [28] R.A. Weismiller, J.L. Ahlrichs, J.L. White, Infrared studies of hydroxy-aluminum
562 interlayer material, Soil Sci. Soc. Amer. Proc. 31 (1967) 459-463.

563 [29] R.D. Harter, J.L. Ahlrichs, Determination of clay surface acidity by infrared
564 spectroscopy, Soil Sci. Soc. Amer. Proc. 31 (1967) 30-33.
565 [30] M. Schnitzer, S.I.M. Skinner, The carbonyl group in a soil organic matter preparation,
566 Soil Sci. Soc. Amer. Proc. 29 (1965) 400-405.
567 [31] S. Brunauer, L.S. Deming, W.E. Deming, E. Teller, On a theory of the van der waals
568 adsorption of gases, J. Am. Chem. Soc. 62 (7) (1940) 1723-1732.
569 [32] D.A. Georgantas, H.P. Grigoropoulou, Orthophosphate and metaphosphate ion removal
570 from aqueous solution using alum and aluminum hydroxide, J. Colloid Interface Sci. 315
571 (1) (2007) 70-79.
572 [33] J.D. Hem, C.E. Roberson, Form and stability of aluminum hydroxide complexes in
573 dilute solution, Chemistry of aluminum in natural water, Geological survey water-supply
574 paper, 1827-A, United States Government Printing office, Washington, USA, 1967.
575 [34] S. Agyin-Birikorang, G.A. O'Connor, Lability of Drinking Water Treatment Residuals
576 (WTR) Immobilized Phosphorus: Aging and pH Effects, J. Environ. Qual. 36 (2007)
577 1076-1085.
578 [35] W. Stumm, J.J. Morgan, Aquatic Chemistry: Chemical equilibria and rate in natural
579 waters (Third edition), A Wiley-interscience Publication, John Wiley & Sons, New York,
580 USA, 1996.
581 [36] K.F.N.K. Kwong, P.M. Huang, Influence of citric acid on the hydrolytic reactions of
582 aluminum, Soil Sci. Soc. Am. J. 41 (1977) 692-697.
583 [37] P.H. Hsu, Formation of gibbsite from aging hydroxy-aluminum solutions, Soil Sci. Soc.
584 Amer. Proc. 30 (1966) 173-176.
585 [38] K.F.N.K. Kwong, P.M. Huang, Sorption of phosphate by hydrolytic reaction products of
586 aluminium, Nature 271 (1978) 336-338.

[39] S.J. Gregg, K.S.W. Sing, Adsorption, surface area and porosity, Academic Press, New York, USA, 1982.

[40] R.S. Mikhail, S. Brunauer, E.E. Bodor, Investigations of a complete pore structure analysis II. Analysis of four silica gels, J. Colloid Interface Sci. 26 (1) (1968) 54-61.

[41] C.J. Gommes, S. Blacher, J.P. Pirard, Nitrogen adsorption on silica xerogels or the odd look of a t plot, Langmuir 21 (5) (2005) 1703-1705.

615

Table 1

The chemical components of the fresh alum sludge (ageing time: 0 day) and the aged alum sludge (ageing time: 6, 12 and 18 months)

Chemical composition	Unit	Amount (mean ± SD)			
		0 day	6 months	12 months	18 months
Moisture content	%	34.59 ± 1.87	24.73 ± 0.52	25.25 ± 1.0	24.58 ± 1.59
Aluminium (as Al_2O_3)	mg g^{-1}-sludge	424.3 ± 2.97	430.4 ± 8.63	418.9 ± 1.44	436.7 ± 1.01
Iron (as Fe_2O_3)	mg g^{-1}-sludge	8.86 ± 0.67	11.00 ± 0.85	9.01 ± 1.30	12.2 ± 0.36
Calcium (as CaO)	mg g^{-1}-sludge	8.77 ± 0.61	11.46 ± 0.51	8.87 ± 0.25	8.32 ± 0.49
Magnesium (as MgO)	mg g^{-1}-sludge	4.11 ± 0.69	7.34 ± 0.31	6.75 ± 0.27	5.77 ± 0.33
Humic acid (as TOC)	mg g^{-1}-sludge	145.1 ± 2.91	101.6 ± 4.17	156.1 ± 1.47	137.3 ± 1.83
Cl^-	mg g^{-1}-sludge	15.89 ± 0.09	15.73 ± 0.47	16.31 ± 0.17	16.41 ± 0.37
SO_4^{2-}	mg g^{-1}-sludge	9.73 ± 0.35	8.57 ± 0.16	8.72 ± 0.19	9.34 ± 0.23
Silicon oxide (as SiO_2)	mg g^{-1}-sludge	27.67 ± 1.90	13.17 ± 0.83	24.01 ± 1.67	27.76 ± 0.94
Mass loss at 500 °C	%	54.96 ± 0.12	50.29 ± 0.43	53.59 ± 0.17	54.85 ± 0.08
Mass loss at 1000 °C	%	0.23 ± 0.01	0.24 ± 0.03	0.24 ± 0.02	0.24 ± 0.02

616

617

618

619

620

621

622

623

624

Table 2

Results of BET plot using nitrogen adsorption isotherm of the fresh alum sludge (ageing time: 0 day) and the aged alum sludges (ageing time: 6, 12 and 18 months)

Ageing time	p/p^0 range	n_m (ml (STP) g^{-1})	BET c-constants	A_{BET} (m^2 g^{-1})	r^2
0 day	0.063-0.280	11.27	59.09	49.03	0.99996
6 months	0.029-0.240	14.33	92.58	62.33	0.99995
12 months	0.045-0.239	12.55	75.84	54.60	0.99996
18 months	0.047-0.200	12.31	79.63	53.54	0.99997

642

Table 3

Harkins-Jura model constants and t_{HJ}-plot results of the fresh alum sludge (ageing time: 0 day) and the aged alum sludges (ageing time: 6, 12 and 18 months)

	HJ model			$A_{t,HJ}$			Mesopore			Micropore
	a	*b*	r^2	p/p^o range	t_{HJ} range (Å)	$A_{t,HJ}$ ($m^2\ g^{-1}$)	p/p^o range	t_{HJ} range (Å)	$A_{t,HJ,Meso}$ ($m^2\ g^{-1}$)	surface area ($m^2\ g^{-1}$)
0 day	0.864	-0.068	0.9996	0.05-0.100	2.96-3.41	48.75	0.32-0.6	5.04-8.40	33.44	15.31
6 months	1.065	0.040	0.9999	0.051-0.080	3.16-3.42	61.79	0.10-0.32	3.58-4.99	62.97	0
12 months	1.041	0.039	0.9998	0.045-0.084	3.07-3.42	53.34	0.10-0.32	3.54-4.94	55.59	0
18 months	1.056	0.048	0.9999	0.039-0.083	3.03-3.42	52.43	0.10-0.32	3.54-4.93	54.45	0

643

644

645

646

647

648

649

650

651

652

653

654

655

656

657

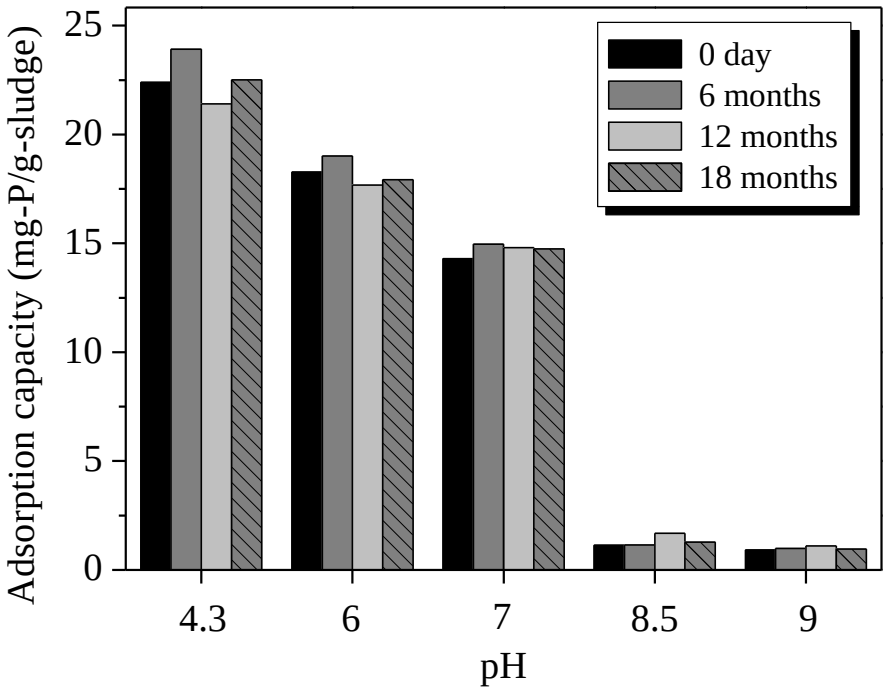

Fig. 1. P adsorption capacity of the alum sludge at different ageing times and pH condition

672

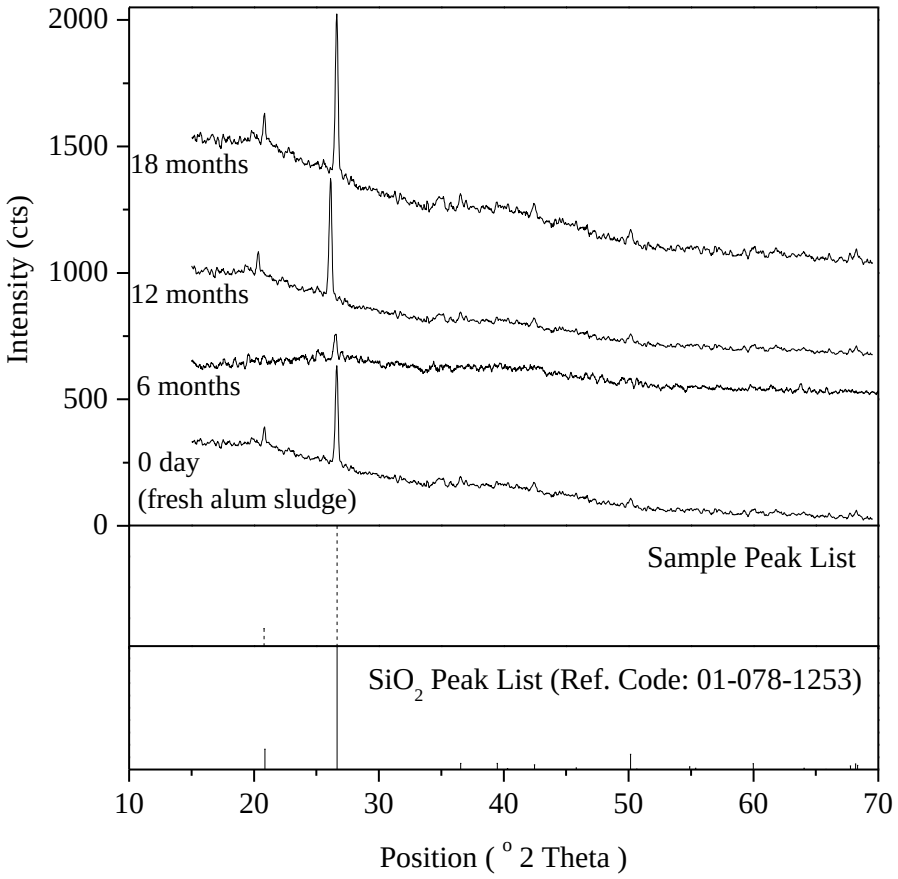

Fig. 2. X-ray diffraction patterns of alum sludge at various ageing times

673

674

675

676

677

678

679

680

681

682

683

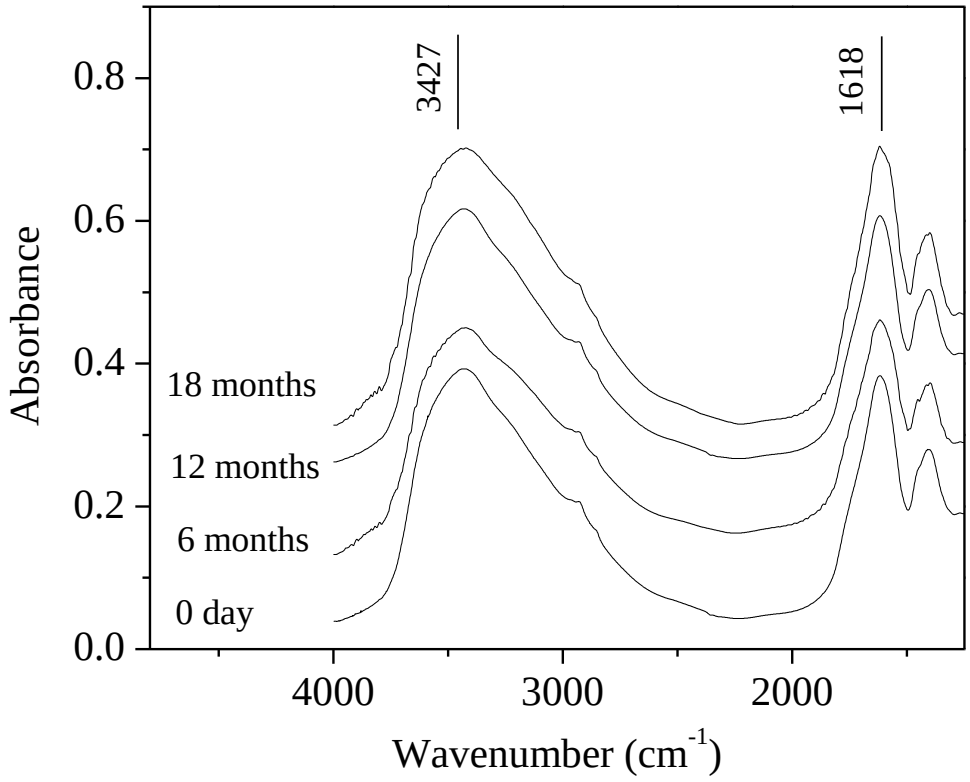

Fig. 3. ATR-FTIR spectra of alum sludge samples with different ageing times

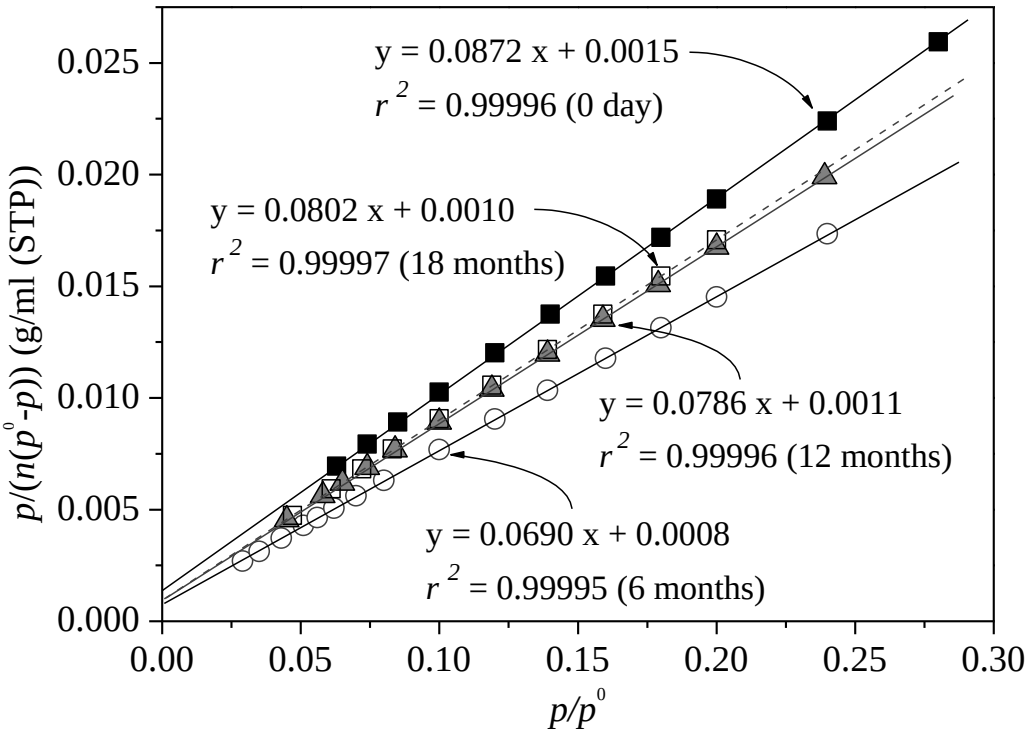

Fig. 4. BET plots of low temperature nitrogen adsorption isotherm of the fresh alum sludge (ageing time: 0 day) and the aged alum sludges (ageing time: 6, 12 and 18 months)

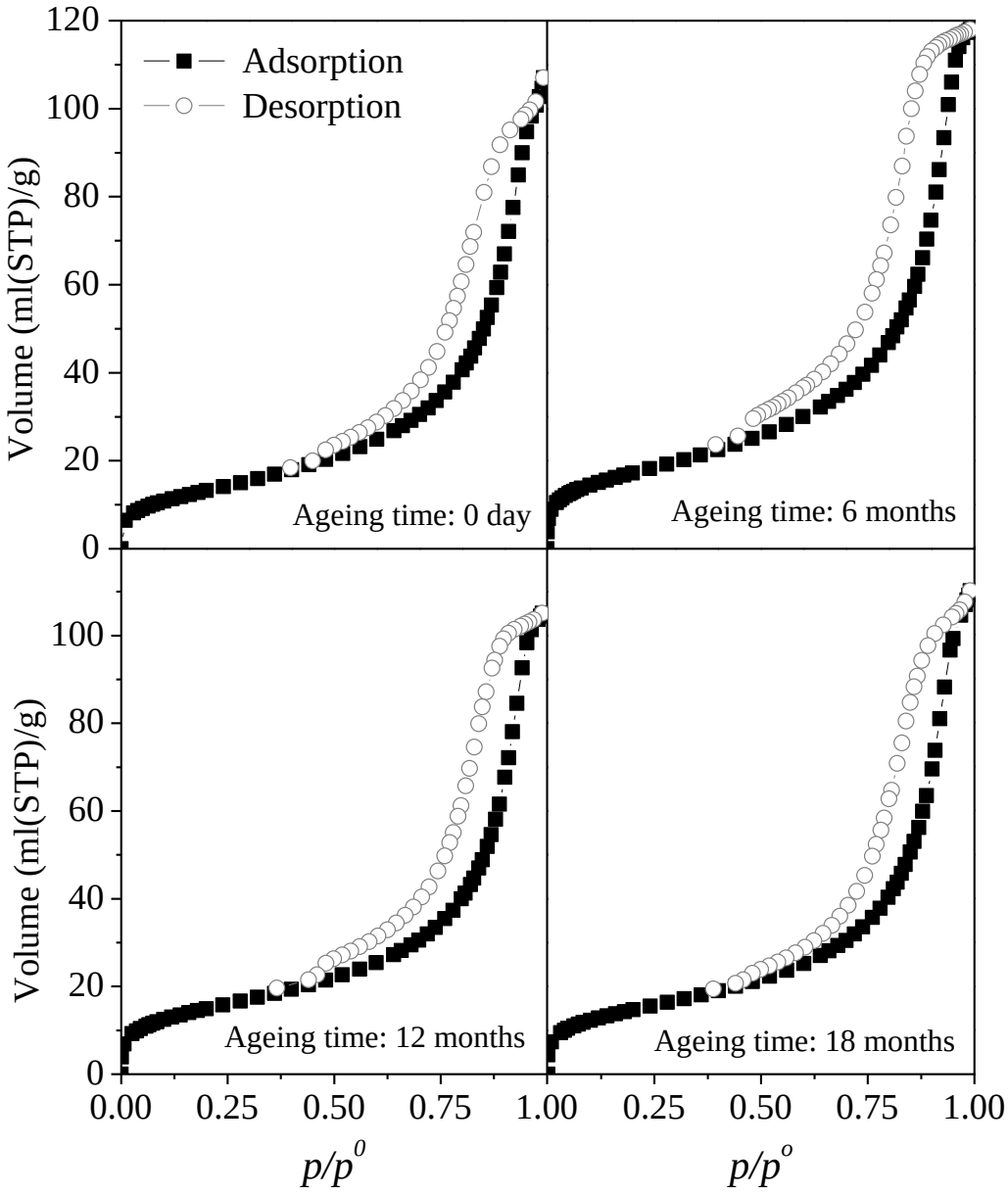

Fig. 5. Nitrogen adsorption-desorption isotherms at 77.4 K for different ageing times of alum sludges

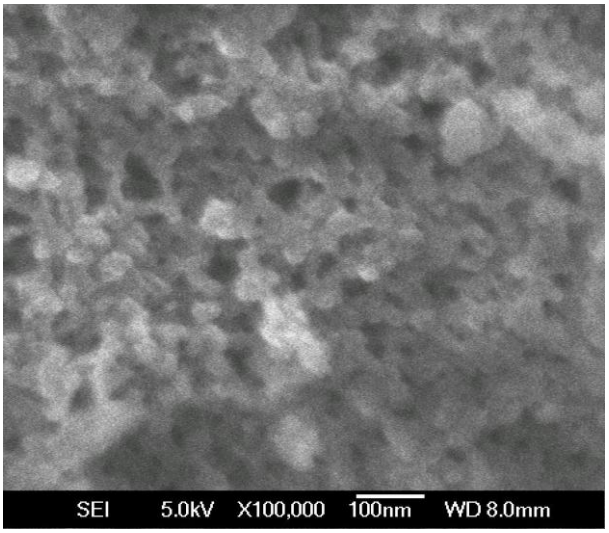

(a) ageing time: 0 day

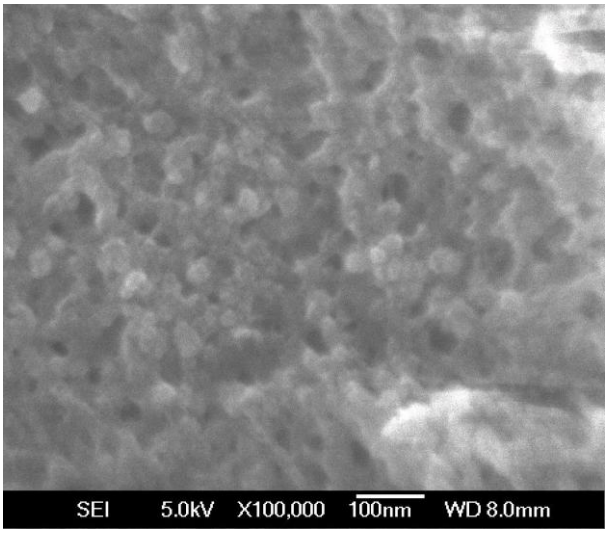

(b) ageing time: 6 months

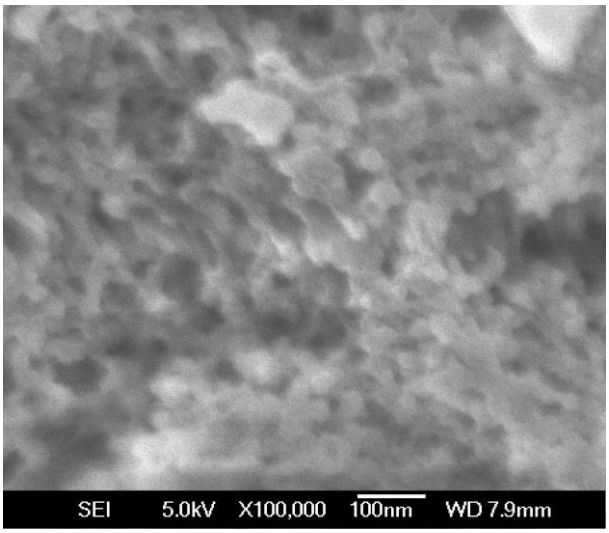

(c) ageing time:12 months

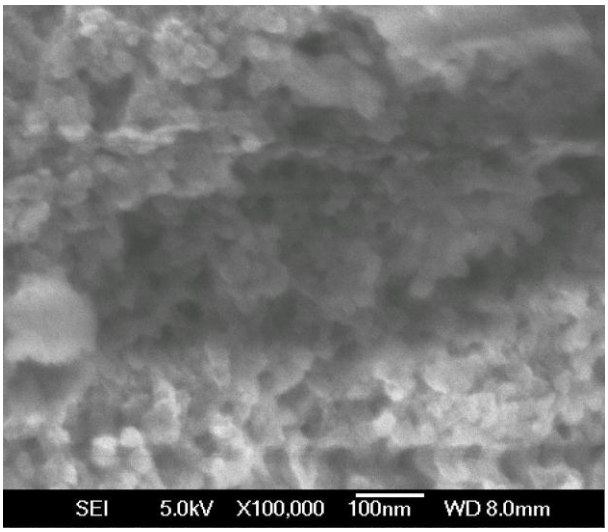

(d) ageing time:18 months

Fig. 6. SEM images of the fresh alum sludge (ageing time: 0 day) and the aged alum sludges (ageing time: 6, 12 and 18 months)

715

716

717

718

719

720

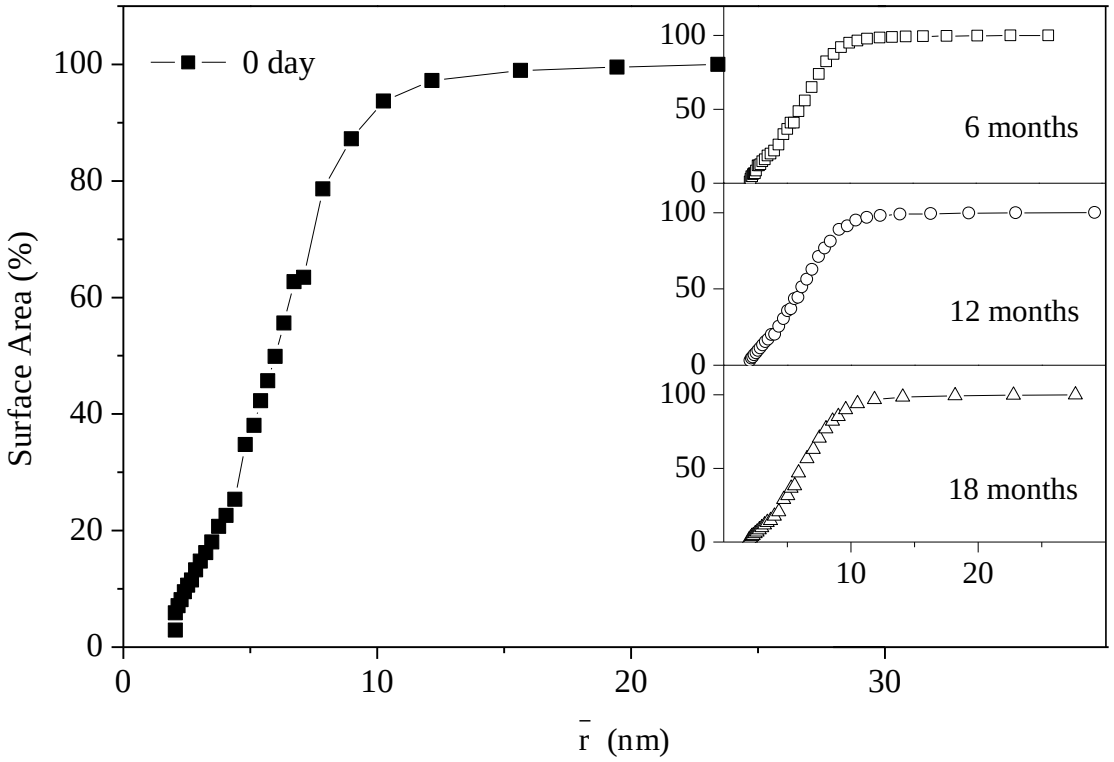

Fig. 7. Mesopore surface area-pore size distribution of the fresh alum sludge (ageing time: 0 day) and the aged alum sludges (ageing time: 6, 12 and 18 months)

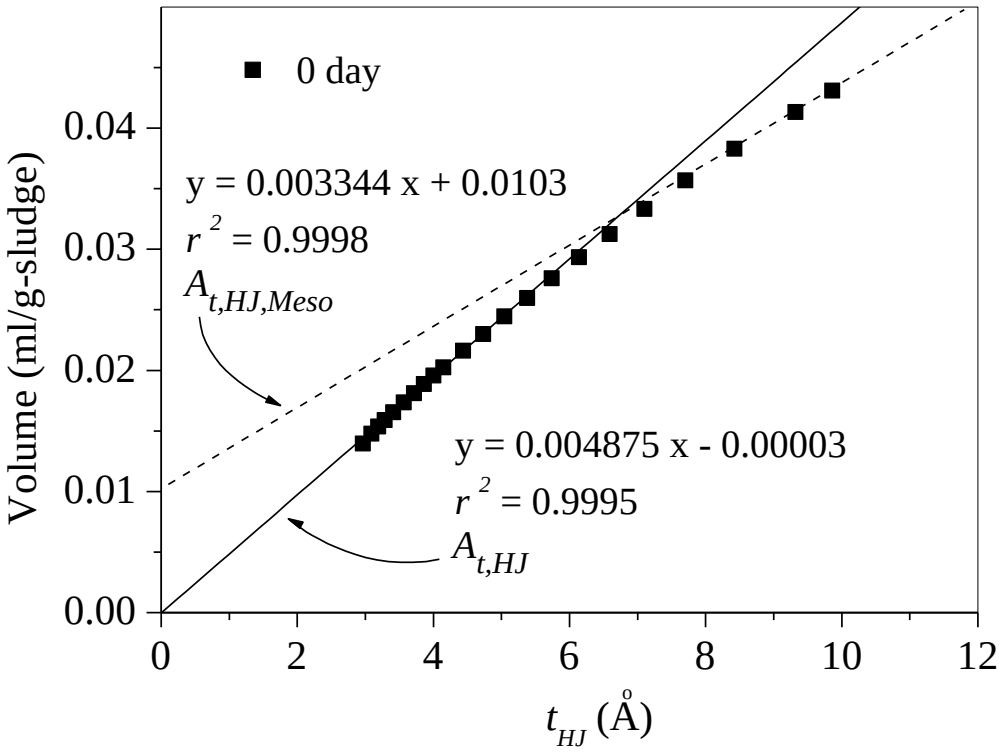

Fig. 8. *t*-plot of the fresh alum sludge (ageing time: 0 day) (using HJ model and HJ *t*-equation)

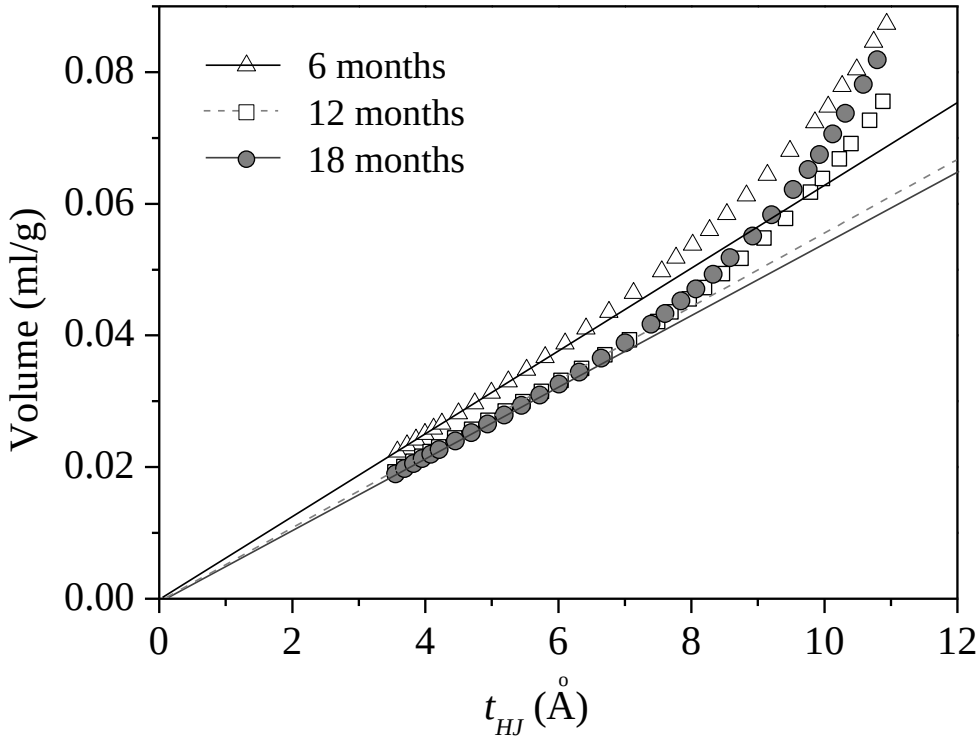

Fig. 9. *t*-plot of 6, 12 and 18 months aged alum sludge (using HJ model and HJ *t*-equation)

745